HHS Public Access

Author manuscript

J Am Chem Soc. Author manuscript; available in PMC 2024 June 28.

Published in final edited form as:

J Am Chem Soc. 2023 June 28; 145(25): 14000–14009. doi:10.1021/jacs.3c03771.

Chemoenzymatic and Synthetic Approaches To Investigate Aspartate- and Glutamate-ADP-Ribosylation

Kyuto Tashiro[‖],
Department of Biochemistry, University of Texas Southwestern Medical Center, Dallas, Texas 75390-9038, United States

Sven Wijngaarden[‖],
Bio-Organic Synthesis, Leiden Institute of Chemistry, Leiden University, 2333 CC Leiden, The Netherlands

Jugal Mohapatra,
Department of Biochemistry, University of Texas Southwestern Medical Center, Dallas, Texas 75390-9038, United States;

Johannes G. M. Rack,
Sir William Dunn School of Pathology, University of Oxford, Oxford OX1 3RE, U.K.

Ivan Ahel,
Sir William Dunn School of Pathology, University of Oxford, Oxford OX1 3RE, U.K.

Dmitri V. Filippov,
Bio-Organic Synthesis, Leiden Institute of Chemistry, Leiden University, 2333 CC Leiden, The Netherlands;

Glen Liszczak
Department of Biochemistry, University of Texas Southwestern Medical Center, Dallas, Texas 75390-9038, United States

Abstract

We report here chemoenzymatic and fully synthetic methodologies to modify aspartate and glutamate side chains with ADP-ribose at specific sites on peptides. Structural analysis of aspartate and glutamate ADP-ribosylated peptides reveals near-quantitative migration of the side chain linkage from the anomeric carbon to the 2″- or 3″-ADP-ribose hydroxyl moieties. We find that this linkage migration pattern is unique to aspartate and glutamate ADP-ribosylation and propose that the observed isomer distribution profile is present in biochemical and cellular environments. After defining distinct stability properties of aspartate and glutamate ADP-ribosylation, we devise methods to install homogenous ADP-ribose chains at specific glutamate

Corresponding Author: Glen Liszczak – Department of Biochemistry, University of Texas Southwestern Medical Center, Dallas, Texas 75390-9038, United States; glen.liszczak@utsouthwestern.edu.

[‖]K.T. and S.W. contributed equally to this work.

Supporting Information

The Supporting Information is available free of charge at https://pubs.acs.org/doi/10.1021/jacs.3c03771.

Additional figures, molecular characterization, materials and methods, and uncropped gels (PDF)

The authors declare no competing financial interest.

sites and assemble glutamate-modified peptides into full-length proteins. By implementing these technologies, we show that histone H2B E2 tri-ADP-ribosylation is able to stimulate the chromatin remodeler ALC1 with similar efficiency to histone serine ADP-ribosylation. Our work reveals fundamental principles of aspartate and glutamate ADP-ribosylation and enables new strategies to interrogate the biochemical consequences of this widespread protein modification.

Graphical Abstract

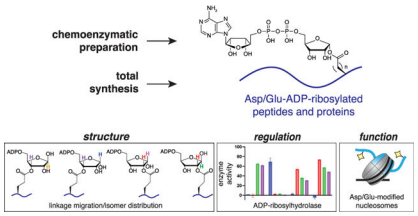

INTRODUCTION

Protein ADP-ribosylation (ADPr) is a dynamic, enzymatically regulated process in which the ADP-ribose moiety from NAD^+ can be deposited onto several side chain functionalities.[1,2] The resulting mono-ADP-ribose modification can directly operate in biochemical signaling cascades or serve as a nucleation site for the formation of protein-linked ADP-ribose polymers.[3,4] To date, hundreds of ADP-ribosylated proteins have been reported to regulate a diverse set of cellular pathways.[5–8] It is now increasingly appreciated that modification site, linkage identity, and ADP-ribose polymer length can cooperate to specify unique biochemical outputs.[2]

Many of the proteins involved in ADPr regulation and function have been identified as therapeutic targets for various human diseases,[9,10] with poly(ADP-ribose) polymerase 1/2 (PARP1/2) inhibitors being successfully employed to treat homology repair-deficient cancers.[11] The translational potential of PARP inhibition has inspired extensive efforts to develop PARP isoform-specific small molecule inhibitors and decipher mechanisms of ADP-ribosyltransferase activity and substrate selectivity.[9,11] More recently, innovative synthetic and chemoenzymatic technologies have been developed to install ADP-ribose at specific sites on synthetic peptides and full-length proteins.[4,12–19] These approaches have been largely focused on serine-ADPr (Ser-ADPr), a DNA damage-induced modification that is catalyzed by the PARP1:HPF1 complex.[20,21] Semisynthetic ADP-ribosylated proteins, including core histones and other chromatin architecture proteins, have been employed to determine important mechanistic principles by which specific Ser-ADPr sites and corresponding polymer chain lengths impact chromatin structure at DNA damage sites.[4,13,14] Serine mono-ADP-ribosylated peptides have also enabled the development of the first site-specific ADP-ribose antibodies.[12] Building upon these successes, strategies to prepare synthetic peptides bearing ADP-ribose at additional side chain functionalities, such as the guanidinium group of arginine, have been recently developed.[16]

Aspartate and glutamate (Asp/Glu) ADP-ribose linkages, which are commonly observed in biological systems, present unique chemical complexities that have prevented the

preparation of homogenously modified molecules. Here, we have developed efficient and scalable chemoenzymatic and fully synthetic strategies to insert ADP-ribose at specific Asp/Glu residues on synthetic peptides. An in-depth characterization of the Asp/Glu-ADP-ribose linkage, including NMR-based structural analysis, revealed rapid and near quantitative migration from the anomeric carbon to the distal ribose 2″ - and 3″-hydroxyl moieties. Additional experiments suggest that the observed isomer distribution profile is a physiological property of Asp/Glu-ADP-ribose. We also employ synthetic peptides bearing ADP-ribose at aspartate, glutamate, arginine, and serine residues to determine unique chemical and enzymatic stability properties of each linkage and their compatibility with commonly employed ADP-ribose detection methods. To gain mechanistic insights into Asp/Glu-ADPr biology, we establish methods to control Asp/Glu-linked ADP-ribose polymer length and assemble Asp/Glu-ADP-ribosylated peptides into full-length proteins. After preparing full-length histone H2B bearing tri-ADP-ribose ($ADPr_3$) at the Glu2 site, we assembled semisynthetic nucleosomes and discovered that histone tail Asp/Glu-poly-ADPr sensitizes nucleosomes to ALC1-dependent chromatin remodeling activity. Our study uncovers the fundamental principles of a well-established posttranslational modification and provides new tools to study Asp/Glu-ADPr-mediated signaling cascades.

RESULTS

Chemoenzymatic Approach To Install Asp/Glu-ADPr on Synthetic Peptides.

Enzyme-based approaches to install ADP-ribose at specific serine side chains on synthetic peptides are highly scalable and compatible with a wide variety of known Ser-ADPr sites.[4,12,14] Chemoenzymatic strategies to generate ADP-ribosylated peptides minimize the use of protection group manipulations by exploiting the inherent chemoselectivity of enzymes and are, therefore, mild and operationally simple. We therefore purified a panel of known ADP-ribosyltransferases with the goal of identifying enzymes that modify side chains other than that of serine on trans-peptide substrates. To be useful for scalable chemoenzymatic preparation of ADP-ribosylated peptides, candidate enzymes must also meet the following criteria: (i) exhibit specificity for a particular amino acid side chain, (ii) convert at least 50% of starting material to ADP-ribosylated product, and (iii) maintain conversion efficiency regardless of the substrate peptide sequence.

We began by incubating two model substrate peptides (100 μM) comprising diverse side chain functionalities with each enzyme and NAD^+ (10 mM) in separate reactions at 25 °C for 30 min. Upon reaction product analysis via reversed-phase high-performance liquid chromatography/mass spectrometry (RP-HPLC/MS), we found that the catalytic domain of PARP14 ($PARP14^{cat}$) efficiently mono-ADP-ribosylates Asp/Glu-containing peptide substrates (Figure 1a,b). Following $PARP14^{cat}$ reaction condition optimization, greater than 50% conversion of the Glu-containing model peptide A (MP^A; sequence: GWTARKSAEVGAGK) to mono-ADP-ribosylated product (denoted as $ADPr_1$) was achieved (Figure 1b). Under all conditions tested, no activity was detected with model peptide B (MP^B; sequence: GWTARKSAQHCAGK), which is devoid of Asp/Glu residues (Figure 1c). Mutational analysis of the MP^A substrate revealed that the E9A mutation abolishes modification of the peptide by $PARP14^{cat}$, while the E9D substitution was

efficiently converted to a mono-ADP-ribosylated product (Figure 1b). Moreover, the addition of a glutamate residue into the MP^B sequence (Q9E) converts this previously inert substrate into a robust substrate for $PARP14^{cat}$ (Figure 1c). Thus, we concluded that $PARP14^{cat}$ efficiently and specifically mono-ADP-ribosylates Asp/Glu side chains on synthetic peptides, which is further supported by previous reports that PARP14 can catalyze Asp/Glu-ADPr.[22]

Enzyme activity screening also revealed that the well-characterized mouse Arg-ADP-ribosyltransferase ARTC2.2[23] efficiently and specifically modifies arginine residues on synthetic peptide substrates (Figures 1a and S2a). Therefore, in addition to Asp/Glu-modified peptides, MP^A constructs bearing Arg- and Ser-$ADPr_1$ were also prepared (via enzymatic modification with ARTC2.2 and the PARP1:HPF1 complex, respectively) and included in characterization experiments throughout this study (Figure S2b). To further confirm linkage identity, modified peptides were incubated with 0.5 M hydroxylamine (NH_2OH) at pH 6.0.[8] As expected, treatment of the MP^A E9$ADPr_1$ peptide with NH_2OH resulted in the replacement of the ADP-ribose adduct with a hydroxamic acid derivative (+15 Da), while the MP^A R5$ADPr_1$ and MP^A S7$ADPr_1$ peptides were unaffected (Figure S3).

Preparation of Peptides Modified at Endogenous Glu-ADPr Sites.

To probe $PARP14^{cat}$ utility in diverse substrate peptide sequence contexts, peptide fragments encompassing various endogenous human Glu-ADPr sites were prepared.[6,24,25] These include $PARP1_{(487–496;\ E488A)}$ E491 ($PARP1_{Frag}$), $H2B_{(1–16)}$ E2 ($H2B_{Frag}$), and linker histone $H1.2_{(1–9)}$ E2 ($H1.2_{Frag}$), all of which were incubated with 100 μM $PARP14^{cat}$ and 10 mM NAD^+ at 25 °C for 30 min. Greater than 50% conversion of each peptide to the mono-ADP-ribosylated product was observed at substrate concentrations up to 0.5 mM (Figure 1d). For each substrate peptide, mutation of the target glutamate residue to alanine abolished $PARP14^{cat}$-dependent ADP-ribosylated product formation (Figure S4). This chemoenzymatic approach was scalable to produce milligram quantities of purified $PARP1_{Frag}$ E491$ADPr_1$, $H2B_{Frag}$ E2$ADPr_1$, and $H1.2_{Frag}$ E2$ADPr_1$ peptides.

Structural Analysis of Asp/Glu-ADP-Ribosylated Peptides.

In the course of substrate peptide mutagenesis analysis, a $PARP1_{Frag}$ construct with an E491D mutation was prepared and ADP-ribosylated with $PARP14^{cat}$. We found that the $PARP1_{Frag,\ E491D}$ D491$ADPr_1$ product elutes from RP-HPLC as two peaks with unique retention times (Figure 2a). Both peaks comprise the expected mass for the $PARP1_{Frag,\ E491D}$ D491$ADPr_1$ product and both are sensitive to the D491A mutation and hydroxylamine treatment (Figures S3 and S5), indicating the occurrence of ADP-ribose linkage migration at the D491 position. It was previously suggested that upon transfer of the ADP-ribose moiety from NAD^+ to the carboxylic acid side chain of glutamate in vitro, acyl migration from the 1″-OH to the 2″-OH position of distal ribose occurs.[26] This is in accordance with (i) our previous attempts to synthesize peptides bearing Glu-ADPr, which revealed indications of such migration after incorporation of a phosphoribosylated glutamic acid building block,[19] and (ii) studies performed on acetyl-ADP-ribose, which report migration

of the acyl functionality between the hydroxyl moieties of the distal ribose.[27] We therefore hypothesized that all Asp/Glu-ADP-ribosylated species contain linkage isomers.

To determine the structure(s) of Asp/Glu-ADPr linkages, the following peptides were analyzed via NMR spectroscopy: (i) $PARP1_{Frag}$ E491$ADPr_1$, (ii) $PARP1_{Frag, E491D}$ D491$ADPr_1$ Peak 1, and (iii) $PARP1_{Frag, E491D}$ D491$ADPr_1$ Peak 2. We note that isomers of the $PARP1_{Frag}$ E491$ADPr_1$ peptide eluted from RP-HPLC as a single peak. Indeed, the $PARP1_{Frag}$ E491$ADPr_1$ ^{1}H-NMR spectrum recorded in D_2O showed four peaks from 5.2 to 5.5 ppm, which could be ascribed to the H1″ protons from four unique isomers of the glutamate:ADP-ribose linkage as assigned by COSY, HSQC, and HMBC experiments (Figures 2b and S29–S31, and Methods for further explanation). Briefly, these signals correspond to ADP-ribose linked via the 2″-OH or 3″-OH of the distal ribose to the glutamate side chain via an ester bond (Figure 2c). Both 2″- and 3″-*O*-Glu-ADPr species also contain a free lactol in which the anomeric hydroxyl could assume either an α- or β-configuration. Thus, the Glu-ADPr peptides contain four distinct linkage isomers, α−2″-, β−2″-, α−3″-, and β−3″-*O*-ADPr, at nearly a 1:1:1:1 ratio as gauged by integration of corresponding H1″-proton resonances (Figure 2c).

As discussed above, the separation of regioisomers via RP-HPLC was observed with aspartate-linked ADP-ribosylated PARP1 peptides. The two distinct $PARP1_{Frag, E491D}$ D491$ADPr_1$ product fractions were isolated after RP-HPLC purification for ^{1}H-NMR analysis. Indeed, each isolated peak showed an excess of a regioisomer, wherein Peak 1 was assigned to the 3″-*O*-Asp ADPr regioisomer and Peak 2 to the 2″-*O*-Asp-ADPr regioisomer (Figures S35–S36). Importantly, the H1″-proton of the α−1″-*O*-Asp ADPr isomer was clearly observed using that HSQC dataset at 6.05 ppm as a minor species (<5%) (Figure S34). A similar analysis was not possible for Glu-ADPr peptides as the H1″ of the α−1″-*O*-Glu-ADPr isomer was overlapping with the H1′ signal of the adenosine found at approximately 6.2 ppm (Figure S30). Also of note, the aldehyde-containing open-chain isomer, which exists in a dynamic equilibrium, was not found in the NMR spectra and is thus present in low abundance. ^{1}H-NMR of $PARP1_{Frag}$ E491$ADPr_1$ and $PARP1_{Frag, E491D}$ D491$ADPr_1$ was also performed under more physiological conditions (PBS buffer, 37 °C, pH = 7.4 in D_2O), which did not greatly alter the ratio of the anomers and regioisomers (Figures S37−S38). This observation hints toward a preponderance of 2″- and 3″-*O*-Glu-ADPr regioisomers in vivo, while the concentrations of 1″-*O*-Glu-ADPr and the open-chain form of Glu-ADPr are low.

Asp/Glu-ADPr Linkage Migration in Biochemical and Cellular Environments.

We next sought to validate that the linkage migration is unique to Asp/Glu-ADPr and occurs in biochemical and cellular environments. Importantly, ribose ring tautomerization, which is dependent upon linkage migration, is accompanied by the formation of an aldehyde at the 1″ position in the ring open state (Figure S6a).[26] The Cohen group has previously demonstrated that this aldehyde readily reacts with aminooxy (AO)-containing chemical probes. To validate probe specificity for migration-prone linkages, an AO-TAMRA probe was incubated with peptides bearing Ser-, Arg-, Asp-, or Glu-ADPr, and reactivity was analyzed via RP-HPLC/MS. Indeed, only aspartate- and glutamate-modified peptides were

labeled with AO-TAMRA as evident from the appearance of the expected peptide mass adduct (+569.4 Da) (Figure S6b).

We next isolated recombinant PARP1 and performed auto-ADPr reactions in the presence of increasing HPF1 concentrations. It is now well-established that HPF1 switches PARP1 automodification activity from Asp/Glu-ADPr to Ser-ADPr.[21] PARP1 (1 μM) and HPF1 (0–25 μM) were incubated with 10 mM NAD^+ and 10 μM stimulating DNA for 20 min at 30 °C and reactions were quenched with 10 μM Olaparib. Reaction mixtures were then incubated with AO-TAMRA for 1 h, quenched with SDS loading dye, and resolved via SDS-PAGE. In-gel fluorescence imaging analysis revealed robust signals ranging from 100 to 250-kDa in the PARP1-only lane, consistent with a wide distribution of poly-ADP-ribose polymer lengths emanating from aspartate and glutamate sites on PARP1 (Figure 2d). Samples were also treated with poly(ADP-ribose) glycohydrolase (PARG), which converts all poly-ADPr sites to mono-ADPr.[28] As expected, a robust fluorescence signal was preserved post-PARG treatment, consistent with the labeling of the side chain-conjugated open ribose ring tautomer (Figure 2d). Identical PARP1 auto-ADPr reactions performed in the presence of 25 μM HPF1 exhibited similar quantitative PARP1 auto-ADPr (Figure 2d). However, AO-probe labeling efficiency decreased by >95% under these conditions. Thus, the HPF1-mediated switch to Ser-ADPr activity also eliminates ADP-ribose linkage migration.

For cell-based analysis of Asp/Glu-ADPr-specific linker migration, we isolated intact nuclei from $HPF1^{-/-}$ HEK293T cells. The NAD^+ cofactor (10 mM) was incubated with intact nuclei for 30 min at 30 °C and reactions were quenched with 10 μM Olaparib. Nuclei were then incubated with AO-TAMRA for 1 h, and nuclear proteins were resolved via SDS-PAGE for in-gel fluorescence imaging analysis. We observed robust AO-TAMRA labeling of proteins throughout the gel molecular weight range, including endogenous PARP1 (Figure 2e). While strong nuclear protein ADPr signal intensity was observed at all HPF1 concentrations tested, the AO-TAMRA signal decreased in an HPF1 concentration-dependent manner and was nearly abolished at the highest HPF1 concentration tested (50 μM) (Figure 2e). These results strongly suggest that the Asp/Glu-ADPr linkage isomers present after enzymatic and synthetic peptide modification are an appropriate representation of Asp/Glu-ADPr in biochemical and cellular samples.

Fully Synthetic Asp/Glu-ADP-Ribosylated Peptides.

To further corroborate the observed regio- and stereochemistry of the enzymatically produced Glu-ADPr and Asp-ADPr peptides, a chemical synthesis of the ADPr-peptides was undertaken. A solid-phase synthesis approach was envisioned based on our previous work toward the chemical synthesis of mono-ADPr-peptides (Figure 3a).[18] In this strategy, sequential on-resin phosphorylation and pyrophosphorylation via phosphoramidite P(III)-P(V) chemistry was performed to generate protected, ADP-ribosylated peptides. Tandem deprotection and purification afforded the desired Asp/Glu-ADP-ribosylated peptides corresponding to various biologically relevant substrates in excellent yield and purity (Figures 3a, S22, and S25–S28). This synthetic approach tolerates a broad range of chemical functionalities in the peptide substrate and is suitable for the future preparation of ADPr-peptides bearing additional unnatural chemical moieties.

The fully synthetic workflow required suitably protected, ribosylated amino acid building blocks, which could be incorporated into a solid-phase peptide synthesis (Figure 3b). Functionalized amino acids contained the ribose 3″- hydroxyl moiety attached to the aspartate or glutamate side chain via an ester linkage. The anomeric ester linkage was not pursued at this step due to issues with its chemical instability and propensity to anomerization.[19,29] However, NMR characterization of the final synthetic ADP-ribosylated peptide shows a mixture of the regioisomers nearly identical to that of the enzymatically modified peptides (Figures S39−S42). Therefore, we confirmed that the distribution of Asp/GluADPr regio- and stereoisomers is thermodynamically controlled under physiological conditions and is independent of the initial location of the ester linkage.

Asp/Glu-ADP-Ribosylated Peptides as Substrates in Biochemical Assays.

Fluorescently labeled MP^A R5ADPr$_1$, MP^A S7ADPr$_1$, MP^A E9ADPr$_1$, and MP^A(E9D) D9ADPr$_1$ constructs were prepared via the chemoenzymatic modification approach to evaluate the influence that linkage identity has on interaction with the Af1521 macrodomain (Figure S7a).[30] A focus was placed on this macrodomain because it serves as a commercially available and commonly utilized pan-ADP-ribose detection reagent (an Af1521 macrodomain-Fc region fusion).[31] A fluorescence polarization-based interaction assay revealed that the Ser-, Asp-, and Glu-linked peptides engage the pan-ADP-ribose detection reagent with similar affinity ($K_{d,app}$ = 1171.4, 1806.0, and 732.1 nM, respectively) (Table 1). Interestingly, the pan-ADP-ribose detection reagent exhibits low nanomolar affinity ($K_{d,app}$ = 15.6 nM) for the MP^A R5ADPr$_1$ peptide. To ensure that this was not due to local sequence variation, we produced the $MP^{A(R5K, E9R)}$ R9ADPr$_1$ construct, which maintained a strong interaction ($K_{d,app}$ = 28.4 nM; Table 1, Figure S7b). Therefore, the pan-ADP-ribose detection reagent exhibits a strong preference for Arg-linked mono-ADP-ribose moieties. This is a particularly important consideration that may introduce bias into common experimental workflows that incorporate the pan-ADPr detection reagent, including immunoprecipitations and western blots.

We have previously shown that PARP1 can be used to elongate ADP-ribose chains from mono-ADP-ribosylated serine sites on synthetic peptides.[4] Following this reaction, peptides with linear polymer chain lengths ranging from 1 to 5 ADP-ribose units could be purified to homogeneity. We wondered if PARP1 would display similar ADP-ribose chain elongation activity with peptide substrates bearing a Glu-ADPr$_1$ modification. Indeed, incubation of MP^A E9ADPr$_1$ with PARP1, stimulating DNA, and NAD^+ resulted in robust ADP-ribose chain elongation, with di-, tri-, and tetra-ADP-ribosylated species being the most abundant products as determined by RP-HPLC/MS analysis (Figure S8a,b). No ADPr activity was detected on unmodified peptides. This workflow enables the preparation of peptides bearing user-defined ADP-ribose chain lengths from specific Asp/Glu sites. Human ADP-ribosylhydrolases are known to selectively hydrolyze certain linkage types, with the MacroD1/D2 enzymes being responsible for reversing Asp/Glu-ADPr.[32] We sought to demonstrate the utility of our Asp/Glu-ADPr-containing peptides in high-throughput ADP-ribosylhydrolase activity assays,[33] which included the enzymes ARH1, ARH3, MacroD1, MacroD2, and PARG.[32,34] As expected, ARH3 and MacroD1/D2 exhibited potent Asp/Glu-ADPr hydrolysis activity (Figure 4a). We note that PARG, while known to be selective

for ribose-ribose bonds, is able to hydrolyze the Asp/Glu-ADPr linkage in the context of the peptide substrates at the concentration tested (1 μM). Additionally, enzyme linkage specificity profiles were largely unaffected by the substrate peptide ADPr method and substrate amino acid sequence. To further probe hydrolase linkage specificity, ARH1/3, MacroD1, and PARG were incubated with Ser-, Arg-, Asp-, or Glu-ADP-ribosylated peptides for 30 min at 25 °C and reactions were analyzed via an RP-HPLC/MS hydrolysis assay. In this assay, ARH1 and MacroD1 exhibited Arg-specific and Asp/Glu-specific ADP-ribosylhydrolase activity, respectively, while ARH3 catalyzed the removal of the ADP-ribose modification from aspartate, glutamate, and serine side chains (Figure S9). Future kinetic and structural analysis with homogenously ADP-ribosylated substrates will be critical to determine the preferred Asp/Glu-ADPr linkage isomer for MacroD1/D2 and ARH3 activity. Overall, integration of homogenously modified peptides into these assay platforms may help to accelerate ongoing ADP-ribosylhydrolase inhibitor discovery efforts.[33,35]

Quantitative Thermal and pH Stability Profiling of Various ADPr Linkages.

Previous work has demonstrated that ADPr thermolability and pH stability can vary based on the linkage type.[36] These are critical parameters to consider when preparing and analyzing ADPr samples. For most ADPr linkage types, stability studies have relied on auto-ADP-ribosylated PARP enzymes wherein modification site(s) and homogeneity cannot be controlled. Additionally, stability analysis has been dependent upon ADPr detection reagents, which can be strongly influenced by linkage type and/or proximal amino acid content. We therefore employed a quantitative RP-HPLC/MS assay to monitor the hydrolysis of homogenously Ser-, Arg-, Asp-, and Glu-ADP-ribosylated peptides under various pH values and temperatures. In line with the earlier studies on the chemical stability of a synthetic Ser-ADPr peptide derived from the N-terminus of H2B,[17] Ser-ADPr demonstrated remarkable stability at high temperatures (37 °C, pH 7.4) and under alkaline conditions (25 °C, pH 9.0), with <5% hydrolysis observed after a 16 h incubation under these conditions (Figure 4b). This is in sharp contrast with Arg-, Asp-, and Glu-ADPr, where near-complete hydrolysis was observed under identical conditions (Figure 4b). Indeed, Asp- and Glu-ADPr were the most heat-sensitive and alkaline pH-sensitive of all linkages tested, with detrimental effects observed at the earliest time-points analyzed under each condition tested. We also subjected all peptides to routine SDS-PAGE sample preparation conditions (1× Laemmli buffer without SDS or dye, 95 °C, 5 min). While modest hydrolysis was observed with Ser-linked ADPr (5%), Arg-, Asp-, and Glu-modified peptides exhibited 48, 62, and 34% hydrolysis, respectively (Figure 4c). Strikingly, >90% of Asp-ADPr was hydrolyzed after 10 min incubation under sample preparation conditions. Thus, common ADPr assay parameters and sample handling conditions may drastically impact results and data interpretation.

Using Semisynthetic Nucleosomes To Investigate Functional Consequences of Histone Glu-ADPr.

ADPr has been reported to target multiple sites on nucleosome-incorporated histones, including serine, aspartate, and glutamate residues.[7,24,37] Many fundamental questions remain regarding the molecular mechanisms through which known nucleosome ADPr sites trigger distinct biochemical signaling outputs. We recently employed semisynthetic,

full-length ADP-ribosylated histones to show that H2BS6- and H3S10-poly-ADPr convert nucleosomes into potent substrates for the ATP-dependent chromatin remodeler ALC1.[4] However, it remains unclear if the well-established H2B E2 ADPr modification similarly stimulates ALC1 or if this output is specific to histone tail serine ADPr. The ALC1 macrodomain engages ADP-ribose chains at least three units in length.[38] We employed a fluorescence polarization-based interaction assay to determine ALC1 macrodomain affinity for glutamate-linked tri-ADP-ribose chains (Figure S7a). Similar to free $ADPr_3$ and serine-linked $ADPr_3$, the ALC1 macrodomain has a high affinity for glutamate-linked $ADPr_3$ ($K_{d,app}$ = 8.4 nM, Figure S10). Thus, linkage identity is not a critical determinant of ALC1 macrodomain binding.

We next sought to prepare semisynthetic nucleosomes bearing the H2B E2$ADPr_3$ modification. We previously established protein chemistry technologies that enable N- and C-terminal ligations of mono- and poly-ADP-ribosylated protein fragments.[4,14] For Glu-ADP-ribosylated peptides, we first prepared a synthetic peptide (H2B amino acids 1–16) with a C-terminal MESNa thioester and performed sequential mono- and poly-ADPr reactions with $PARP14^{cat}$ and PARP1, respectively (Figure 5a). Peptides modified with H2B E2$ADPr_3$ were isolated via RP-HPLC (Figure S11). Having determined the thermal- and alkaline-sensitivity parameters of Asp/Glu ADPr, unique protein chemistry strategies were required to ligate the modified peptide to the recombinant H2B fragment (amino acids 17–135, A17C). Most importantly, ligations were performed at 25 °C for no more than 30 min in an aqueous solution buffered at pH 6.8–7.0. After screening small molecule thiol additives, we found that MPAA afforded the most generous ligation yields (>80%) under these conditions (Figure 5a). Following RP/HPLC purification of the ligation product, the full-length H2B E2$ADPr_3$ product was >95% pure as judged by RP-HPLC/MS characterization (Figure 5b).

The full-length H2B E2$ADPr_3$ protein was assembled into histone octamers as previously described.[4] Subsequent nucleosome assembly was performed with a modified 601 DNA construct compatible with a restriction enzyme accessibility (REA)-based chromatin remodeling assay. We note partial hydrolysis of the nucleosome-incorporated H2B E2$ADPr_3$ modification was observed by 5% TBE native gel analysis (Figures S12 and S13), which was expected given that octamer and nucleosome preparation require overnight incubations under aqueous conditions at pH 7.4. Nucleosomes bearing the H2B E2$ADPr_3$ modification were next employed as substrates in ALC1 chromatin remodeling time course assays, and remodeling-dependent 601 DNA cleavage was visualized on a TBE gel and quantified via densitometry (Figures S14 and S15). Robust ALC1 remodeling activity was observed with H2B E2$ADPr_3$ nucleosomes and rate constant analysis revealed that the H2B E2$ADPr_3$ modification ($k_{remodeling}$ relative to unmodified = 88.2) and the H3 S10$ADPr_3$ modification ($k_{remodeling}$ relative to unmodified = 91.9) activate ALC1 with similar potency (Figures 5c and S15). Unlike ALC1, the chromatin remodeler CHD4 exhibits detectable activity with wild-type nucleosome substrates in our assay (Figures S15 and S16). However, CHD4 does not distinguish between unmodified, H3 S10$ADPr_3$, and H2B E2$ADPr_3$-modified nucleosome substrates. These data demonstrate that histone tail poly-ADPr does not broadly sensitize nucleosomes to remodeling but rather specifically recruits and activates ALC1.

Furthermore, ALC1 is able to efficiently recognize nucleosome substrates that are modified at different types of amino acids on histone tails.

DISCUSSION

Technologies to prepare homogenously ADP-ribosylated proteins have led to key discoveries related to Ser-ADPr and its role in cellular signaling. Inspired by these studies, we have developed chemoenzymatic and fully synthetic routes to install the ADP-ribose moiety onto aspartate and glutamate residues on synthetic peptides. Our methods are highly scalable, provide well-defined material, and are compatible with downstream applications, including modified peptide structure analyses, protein ligation technologies, and other biochemical applications.

The PARP14^{cat} construct employed here matches all critical criteria for our chemoenzymatic peptide ADPr workflow. PARP14^{cat} specifically targets Asp/Glu side chain functionalities, exhibits no overt substrate sequence motif requirements, converts a majority of each substrate peptide to the ADP-ribosylated product, and can be purified in large quantities (>10 mg/L) from an *Escherichia coli* expression system. We note that our application of PARP14^{cat} should not be used to draw conclusions about the biological function of PARP14, which may have a different substrate specificity profile as a full-length protein and in the context of biologically relevant concentrations. Similarly, we have shown that ARTC2.2 is an effective enzymatic tool to prepare peptides that are homogenously ADP-ribosylated at arginine sites. Last, PARP1-catalyzed ADP-ribose chain elongation from mono-ADP-ribosylated peptides (an in *trans* reaction) is far less efficient than chain elongation in the auto-ADPr process. This is because auto-ADPr occurs via an in *cis* reaction or a stimulating DNA-induced PARP1 dimer,[39] both of which result in the formation of long, PARP1-linked ADPr chains and rapid consumption of NAD^+. Therefore, in the event that peptide-linked ADP-ribose chains greater than 5 units in length are required, altered reaction conditions or subsequent rounds of chain elongation from poly-ADP-ribosylated peptide substrates can be employed as we have shown previously.[14]

Asp/Glu-ADPr linkage migration is an area of great interest that has important implications for the regulation, function, and stability of the modification. Interestingly, ^{1}H-NMR spectra reveal less than 5% of the product is modified at the anomeric carbon position. The remaining Asp/Glu-ADP-ribose linkage is equally distributed between the 2″- and 3″-ADP-ribose hydroxyl moieties, each of which is in equilibrium between the alpha- and beta-lactol. That enzyme-based and synthetic methods show nearly identical NMR spectra in multiple sequence contexts strongly suggest that this isomer distribution profile is a fundamental property of Asp/Glu-ADPr. We and others have also observed Asp/Glu-linkage isomers in a cellular context and found that linkage migration in these assays is not dependent upon ADP-ribosyltransferase identity but rather only dependent on the linkage type.

In the future, it will be important to determine the linkage isomer specificity for Asp/Glu-ADP-ribosylhydrolase enzymes. Our assays show that ARH3 is able to hydrolyze Ser-ADPr and Asp/Glu-ADPr, while MacroD1/D2 is specific for Asp/Glu-ADPr. Considering that ADP-ribose is attached to serine exclusively via the anomeric carbon, it is possible

that ARH3 and MacroD1/D2 target different Asp/Glu-ADPr linkage isomers. The tools developed here will be instrumental for the biophysical and structural interrogation of ADP-ribosylhydrolase function and have clear implications for ADP-ribosylhydrolase inhibitor development efforts.

The Asp/Glu-ADPr linkage structure, regulation, and stability properties reported herein should also serve as a critical reference when designing unbiased workflows to study ADPr in cellular and biochemical assays. Indeed, this information proved essential to develop native chemical ligation protocols compatible with Asp/Glu-ADPr. We have also found that the Af1521 macrodomain exhibits a strong preference for the Arg-ADPr linkage over that of serine, aspartate, and glutamate. Thus, reader domain linkage specificity may offer one avenue for linkage-dependent biology and should be similarly interrogated with other known ADPr-binding modules. Moving forward, we envision that semisynthetic ADP-ribosylated proteins will continue to enable the study of Asp/Glu-, Ser-, and Arg-ADPr and their ability to elicit specific biochemical signaling events. With chemical access to Asp/Glu-ADPr now available, staple biochemical and biological tools, including site-specific Asp/Glu-ADPr antibodies, can now be developed to probe this modification in physiology and disease.

Supplementary Material

Refer to Web version on PubMed Central for supplementary material.

ACKNOWLEDGMENTS

G.L. is funded by the National Institute of General Medical Science (1R35GM147140), the Welch Foundation (I-2039-2020040 and I-2039-20230405), and the American Heart Association (937595), and the Cancer Prevention and Research Institute of Texas (RR180051). We thank members of the Michael Cohen lab and the Liszczak lab for helpful discussions. Work in the Ivan Ahel Laboratory is supported by the Biotechnology and Biological Sciences Research Council (BB/R007195/1 and BB/W016613/1), the Wellcome Trust (210634 and 223107), and by Ovarian Cancer Research Alliance (813369).

ABBREVIATIONS

ADP-ribose	adenosine diphosphate ribose
ADPr	ADP-ribosylation
ALC1	amplified in liver cancer 1
AO-TAMRA	aminooxy tetramethylrhodamine
ARH1	ADP-ribosylhydrolase 1
ARH3	ADP-ribosylhydrolase 3
ARTC2.2	ADP-ribosyltransferase C2
CHD4	chromodomain helicase DNA-binding protein 4
H2B	histone H2B
H3	histone H3

HPF1	histone PARylation factor 1
MacroD1	macrodomain-containing protein 1
MacroD2	macrodomain-containing protein 2
MESNa	sodium 2-mercaptoethanefulfonate
MP^A	model peptide A
MP^B	model peptide B
MPAA	4-mercaptophenylacetic acid
NAD^+	nicotinamide adenine dinucleotide
PARG	poly(ADP-ribose) glycohydrolase
PARP	poly(ADP-ribose) polymerase

REFERENCES

(1). Gupte R; Liu Z; Kraus WL PARPs and ADP-ribosylation: recent advances linking molecular functions to biological outcomes. Genes Dev. 2017, 31, 101–126. [PubMed: 28202539]

(2). Luscher B; Ahel I; Altmeyer M; Ashworth A; Bai P; Chang P; Cohen M; Corda D; Dantzer F; Daugherty MD; et al. ADP-ribosyltransferases, an update on function and nomenclature. FEBS J. 2022, 289, 7399–7410. [PubMed: 34323016]

(3). (a)Langelier MF; Billur R; Sverzhinsky A; Black BE; Pascal JM HPF1 dynamically controls the PARP1/2 balance between initiating and elongating ADP-ribose modifications. Nat. Commun 2021, 12, 6675. [PubMed: 34795260] (b)Prokhorova E; Agnew T; Wondisford AR; Tellier M; Kaminski N; Beijer D; Holder J; Groslambert J; Suskiewicz MJ; Zhu K; et al. Unrestrained poly-ADP-ribosylation provides insights into chromatin regulation and human disease. Mol. Cell 2021, 81, 2640–2655.e8. [PubMed: 34019811]

(4). Mohapatra J; Tashiro K; Beckner RL; Sierra J; Kilgore JA; Williams NS; Liszczak G Serine ADP-ribosylation marks nucleosomes for ALC1-dependent chromatin remodeling. Elife 2021, 10, No. e71502. [PubMed: 34874266]

(5). Daniels CM; Ong SE; Leung AK The Promise of Proteomics for the Study of ADP-Ribosylation. Mol. Cell 2015, 58, 911–924. [PubMed: 26091340]

(6). Hendriks IA; Buch-Larsen SC; Prokhorova E; Elsborg JD; Rebak A; Zhu K; Ahel D; Lukas C; Ahel I; Nielsen ML The regulatory landscape of the human HPF1- and ARH3-dependent ADP-ribosylome. Nat. Commun 2021, 12, 5893. [PubMed: 34625544]

(7). Leidecker O; Bonfiglio JJ; Colby T; Zhang Q; Atanassov I; Zaja R; Palazzo L; Stockum A; Ahel I; Matic I Serine is a new target residue for endogenous ADP-ribosylation on histones. Nat. Chem. Biol 2016, 12, 998–1000. [PubMed: 27723750]

(8). Zhang Y; Wang J; Ding M; Yu Y Site-specific characterization of the Asp- and Glu-ADP-ribosylated proteome. Nat. Methods 2013, 10, 981–984. [PubMed: 23955771]

(9). Challa S; Stokes MS; Kraus WL MARTs and MARylation in the Cytosol: Biological Functions, Mechanisms of Action, and Therapeutic Potential. Cell 2021, 10, 313.

(10). Palazzo L; Mikolcevic P; Mikoc A; Ahel I ADP-ribosylation signalling and human disease. Open Biol. 2019, 9, No. 190041. [PubMed: 30991935]

(11). Lord CJ; Ashworth A PARP inhibitors: Synthetic lethality in the clinic. Science 2017, 355, 1152–1158. [PubMed: 28302823]

(12). Bonfiglio JJ; Leidecker O; Dauben H; Longarini EJ; Colby T; San Segundo-Acosta P; Perez KA; Matic I An HPF1/PARP1-Based Chemical Biology Strategy for Exploring ADP-Ribosylation. Cell 2020, 183, 1086–1102.e23. [PubMed: 33186521]

(13). Hananya N; Daley SK; Bagert JD; Muir TW Synthesis of ADP-Ribosylated Histones Reveals Site-Specific Impacts on Chromatin Structure and Function. J. Am. Chem. Soc 2021, 143, 10847–10852. [PubMed: 34264659]

(14). Tashiro K; Mohapatra J; Brautigam CA; Liszczak G A Protein Semisynthesis-Based Strategy to Investigate the Functional Impact of Linker Histone Serine ADP-Ribosylation. ACS Chem. Biol 2022, 17, 810–815. [PubMed: 35312285]

(15). van der Heden van Noort GJ; van der Horst MG; Overkleeft HS; van der Marel GA; Filippov DV Synthesis of mono-ADP-ribosylated oligopeptides using ribosylated amino acid building blocks. J. Am. Chem. Soc 2010, 132, 5236–5240. [PubMed: 20232863]

(16). Voorneveld J; Kloet MS; Wijngaarden S; Kim RQ; Moutsiopoulou A; Verdegaal M; Misra M; Dikic I; van der Marel GA; Overkleeft HS; et al. Arginine ADP-Ribosylation: Chemical Synthesis of Post-Translationally Modified Ubiquitin Proteins. J. Am. Chem. Soc 2022, 144, 20582–20589. [PubMed: 36318515]

(17). Voorneveld J; Rack JGM; Ahel I; Overkleeft HS; van der Marel GA; Filippov DV Synthetic alpha- and beta-Ser-ADP-ribosylated Peptides Reveal alpha-Ser-ADPr as the Native Epimer. Org. Lett 2018, 20, 4140–4143. [PubMed: 29947522]

(18). Voorneveld J; Rack JGM; van Gijlswijk L; Meeuwenoord NJ; Liu Q; Overkleeft HS; van der Marel GA; Ahel I; Filippov DV Molecular Tools for the Study of ADP-Ribosylation: A Unified and Versatile Method to Synthesise Native Mono-ADP-Ribosylated Peptides. Chem. – Eur. J 2021, 27, 10621–10627. [PubMed: 33769608]

(19). Kistemaker HA; Nardozza AP; Overkleeft HS; van der Marel GA; Ladurner AG; Filippov DV Synthesis and Macrodomain Binding of Mono-ADP-Ribosylated Peptides. Angew. Chem. Int. Ed 2016, 55, 10634–10638.

(20). Bonfiglio JJ; Fontana P; Zhang Q; Colby T; Gibbs-Seymour I; Atanassov I; Bartlett E; Zaja R; Ahel I; Matic I Serine ADP-Ribosylation Depends on HPF1. Mol. Cell 2017, 65, 932–940.e6. [PubMed: 28190768]

(21). Gibbs-Seymour I; Fontana P; Rack JGM; Ahel I HPF1/C4orf27 Is a PARP-1-Interacting Protein that Regulates PARP-1 ADP-Ribosylation Activity. Mol. Cell 2016, 62, 432–442. [PubMed: 27067600]

(22). Wallace SR; Chihab LY; Yamasaki M; Yoshinaga BT; Torres YM; Rideaux D; Javed Z; Turumella S; Zhang M; Lawton DR; et al. Rapid Analysis of ADP-Ribosylation Dynamics and Site-Specificity Using TLC-MALDI. ACS Chem. Biol 2021, 16, 2137–2143. [PubMed: 34647721]

(23). (a)Kanaitsuka T; Bortell R; Stevens LA; Moss J; Sardinha D; Rajan TV; Zipris D; Mordes JP; Greiner DL; Rossini AA Expression in BALB/c and C57BL/6 mice of Rt6-1 and Rt6-2 ADP-ribosyltransferases that differ in enzymatic activity: C57BL/6 Rt6-1 is a natural transferase knockout. J. Immunol 1997, 159, 2741–2749. [PubMed: 9300695] (b)Mueller-Dieckmann C; Ritter H; Haag F; Koch-Nolte F; Schulz GE Structure of the ecto-ADP-ribosyl transferase ART2.2 from rat. J. Mol. Biol 2002, 322, 687–696. [PubMed: 12270706] (c)Ritter H; Koch-Nolte F; Marquez VE; Schulz GE Substrate binding and catalysis of ecto-ADP-ribosyltransferase 2.2 from rat. Biochemistry 2003, 42, 10155–10162. [PubMed: 12939142]

(24). Ogata N; Ueda K; Hayaishi O ADP-ribosylation of histone H2B. Identification of glutamic acid residue 2 as the modification site. J. Biol. Chem 1980, 255, 7610–7615. [PubMed: 7400135]

(25). Ogata N; Ueda K; Kagamiyama H; Hayaishi O ADP-ribosylation of histone H1. Identification of glutamic acid residues 2, 14, and the COOH-terminal lysine residue as modification sites. J. Biol. Chem 1980, 255, 7616–7620. [PubMed: 6772638]

(26). Morgan RK; Cohen MS A Clickable Aminooxy Probe for Monitoring Cellular ADP-Ribosylation. ACS Chem. Biol 2015, 10, 1778–1784. [PubMed: 25978521]

(27). (a)Jackson MD; Denu JM Structural identification of 2′- and 3’-O-acetyl-ADP-ribose as novel metabolites derived from the Sir2 family of beta-NAD+-dependent histone/protein deacetylases. J. Biol. Chem 2002, 277, 18535–18544. [PubMed: 11893743] (b)Sauve AA; Celic I; Avalos J; Deng H; Boeke JD; Schramm VL Chemistry of gene silencing: the mechanism of NAD+-dependent deacetylation reactions. Biochemistry 2001, 40, 15456–15463. [PubMed: 11747420]

(28). Slade D; Dunstan MS; Barkauskaite E; Weston R; Lafite P; Dixon N; Ahel M; Leys D; Ahel I The structure and catalytic mechanism of a poly(ADP-ribose) glycohydrolase. Nature 2011, 477, 616–620. [PubMed: 21892188]

(29). Kistemaker HA; van Noort GJ; Overkleeft HS; van der Marel GA; Filippov DV Stereoselective ribosylation of amino acids. Org. Lett 2013, 15, 2306–2309. [PubMed: 23614697]

(30). Allen MD; Buckle AM; Cordell SC; Lowe J; Bycroft M The crystal structure of AF1521 a protein from Archaeoglobus fulgidus with homology to the non-histone domain of macroH2A. J. Mol. Biol 2003, 330, 503–511. [PubMed: 12842467]

(31). Gibson BA; Conrad LB; Huang D; Kraus WL Generation and Characterization of Recombinant Antibody-like ADP-Ribose Binding Proteins. Biochemistry 2017, 56, 6305–6316. [PubMed: 29053245]

(32). Rosenthal F; Feijs KL; Frugier E; Bonalli M; Forst AH; Imhof R; Winkler HC; Fischer D; Caflisch A; Hassa PO; Lüscher B; Hottiger MO Macrodomain-containing proteins are new mono-ADP-ribosylhydrolases. Nat. Struct. Mol. Biol 2013, 20, 502–507. [PubMed: 23474714]

(33). Rack JGM; Ahel I A Simple Method to Study ADP-Ribosylation Reversal: From Function to Drug Discovery. Methods Mol. Biol 2023, 2609, 111–132. [PubMed: 36515833]

(34). (a)Abplanalp J; Leutert M; Frugier E; Nowak K; Feurer R; Kato J; Kistemaker HVA; Filippov DV; Moss J; Caflisch A; et al. Proteomic analyses identify ARH3 as a serine mono-ADP-ribosylhydrolase. Nat. Commun 2017, 8, 2055. [PubMed: 29234005] (b)Barkauskaite E; Brassington A; Tan ES; Warwicker J; Dunstan MS; Banos B; Lafite P; Ahel M; Mitchison TJ; Ahel I; et al. Visualization of poly(ADP-ribose) bound to PARG reveals inherent balance between exo- and endo-glycohydrolase activities. Nat. Commun 2013, 4, 2164. [PubMed: 23917065] (c)Brochu G; Duchaine C; Thibeault L; Lagueux J; Shah GM; Poirier GG Mode of action of poly(ADP-ribose) glycohydrolase. Biochim. Biophys. Acta 1994, 1219, 342–350. [PubMed: 7918631] (d)Fontana P; Bonfiglio JJ; Palazzo L; Bartlett E; Matic I; Ahel I Serine ADPribosylation reversal by the hydrolase ARH3. Elife 2017, 6, No. e28533. [PubMed: 28650317] (e)Moss J; Jacobson MK; Stanley SJ Reversibility of arginine-specific mono(ADP-ribosyl)ation: identification in eryth-rocytes of an ADP-ribose-L-arginine cleavage enzyme. Proc. Natl. Acad. Sci. U. S. A 1985, 82, 5603–5607. [PubMed: 2994036]

(35). (a)Dasovich M; Zhuo J; Goodman JA; Thomas A; McPherson RL; Jayabalan AK; Busa VF; Cheng SJ; Murphy BA; Redinger KR; et al. High-Throughput Activity Assay for Screening Inhibitors of the SARS-CoV-2 Mac1 Macrodomain. ACS Chem. Biol 2022, 17, 17–23. [PubMed: 34904435] (b)Rack JGM; Palazzo L; Ahel I (ADP-ribosyl)hydrolases: structure, function, and biology. Genes Dev. 2020, 34, 263–284. [PubMed: 32029451] (c)Gahbauer S; Correy GJ; Schuller M; Ferla MP; Doruk YU; Rachman M; Wu T; Diolaiti M; Wang S; Neitz RJ; et al. Iterative computational design and crystallographic screening identifies potent inhibitors targeting the Nsp3 macrodomain of SARS-CoV-2. Proc. Natl. Acad. Sci. U. S. A 2023, 120, No. e2212931120.(d)Rack JGM; Zorzini V; Zhu Z; Schuller M; Ahel D; Ahel I Viral macrodomains: a structural and evolutionary assessment of the pharmacological potential. Open Biol. 2020, 10, No. 200237. [PubMed: 33202171]

(36). (a)Rodriguez KM; Buch-Larsen SC; Kirby IT; Siordia IR; Hutin D; Rasmussen M; Grant DM; David LL; Matthews J; Nielsen ML; Cohen MS Chemical genetics and proteome-wide site mapping reveal cysteine MARylation by PARP-7 on immune-relevant protein targets. Elife 2021, 10, No. e60480. [PubMed: 33475084] (b)Weixler L; Ikenga NJ; Voorneveld J; Aydin G; Bolte TM; Momoh J; Butepage M; Golzmann A; Luscher B; Filippov DV; et al. Protein and RNA ADP-ribosylation detection is influenced by sample preparation and reagents used. Life Sci. Alliance 2023, 6, No. e202201455.

(37). Huang D; Camacho CV; Martire S; Nagari A; Setlem R; Gong X; Edwards AD; Chiu SP; Banaszynski LA; Kraus WL Oncohistone Mutations Occur at Functional Sites of Regulatory ADP-Ribosylation. Cancer Res. 2022, 82, 2361–2377. [PubMed: 35472077]

(38). Singh HR; Nardozza AP; Moller IR; Knobloch G; Kistemaker HAV; Hassler M; Harrer N; Blessing C; Eustermann S; Kotthoff C; et al. A Poly-ADP-Ribose Trigger Releases the Auto-Inhibition of a Chromatin Remodeling Oncogene. Mol. Cell 2017, 68, 860–871.e7. [PubMed: 29220653]

(39). Eustermann S; Wu WF; Langelier MF; Yang JC; Easton LE; Riccio AA; Pascal JM; Neuhaus D Structural Basis of Detection and Signaling of DNA Single-Strand Breaks by Human PARP-1. Mol. Cell 2015, 60, 742–754. [PubMed: 26626479]

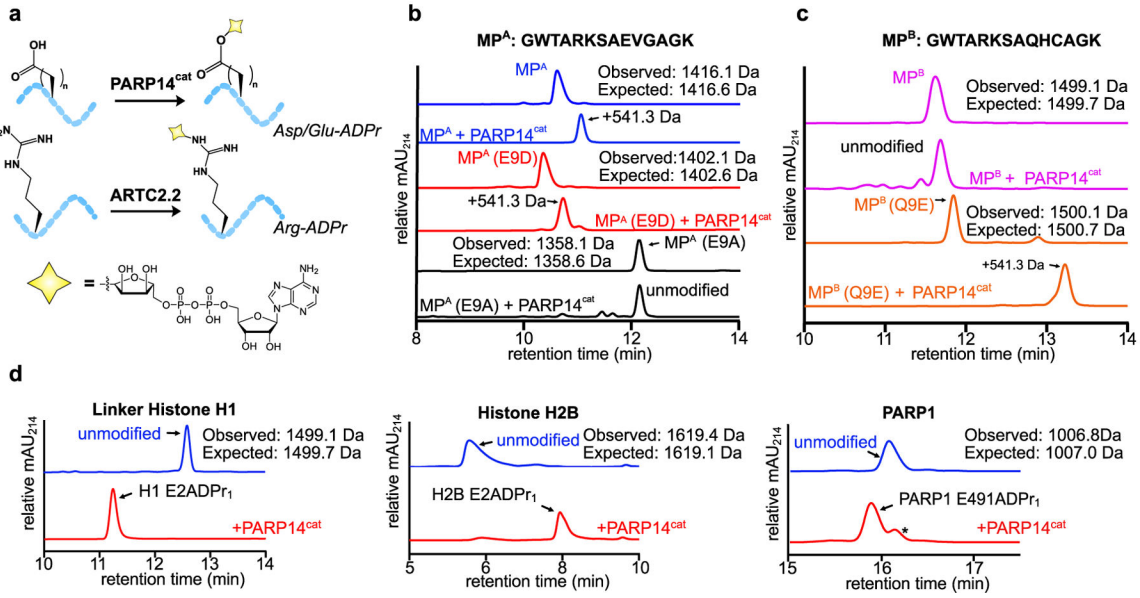

Figure 1.

Chemoenzymatic generation of Asp- and Glu-ADP-ribosylated peptides. (a) Schematic depicting enzyme-catalyzed installation of mono-ADPr at Asp/Glu- and Arg-side chains on synthetic peptides via PARP14^{cat} and ARTC2.2, respectively. (b) RP-HPLC/MS analysis of model peptide MP^{A} and mutant thereof pre- and postincubation with PARP14^{cat}. Note: mono-ADP-ribose adduct = 541.3 Da. (c) As in (b) but with model peptide MP^{B}. (d) RP-HPLC/MS analysis of peptides containing endogenous Glu-ADPr sites pre- and postincubation with PARP14^{cat}. All intact ESI-MS analyses are shown in Figures S1 and S4. *unmodified peptide.

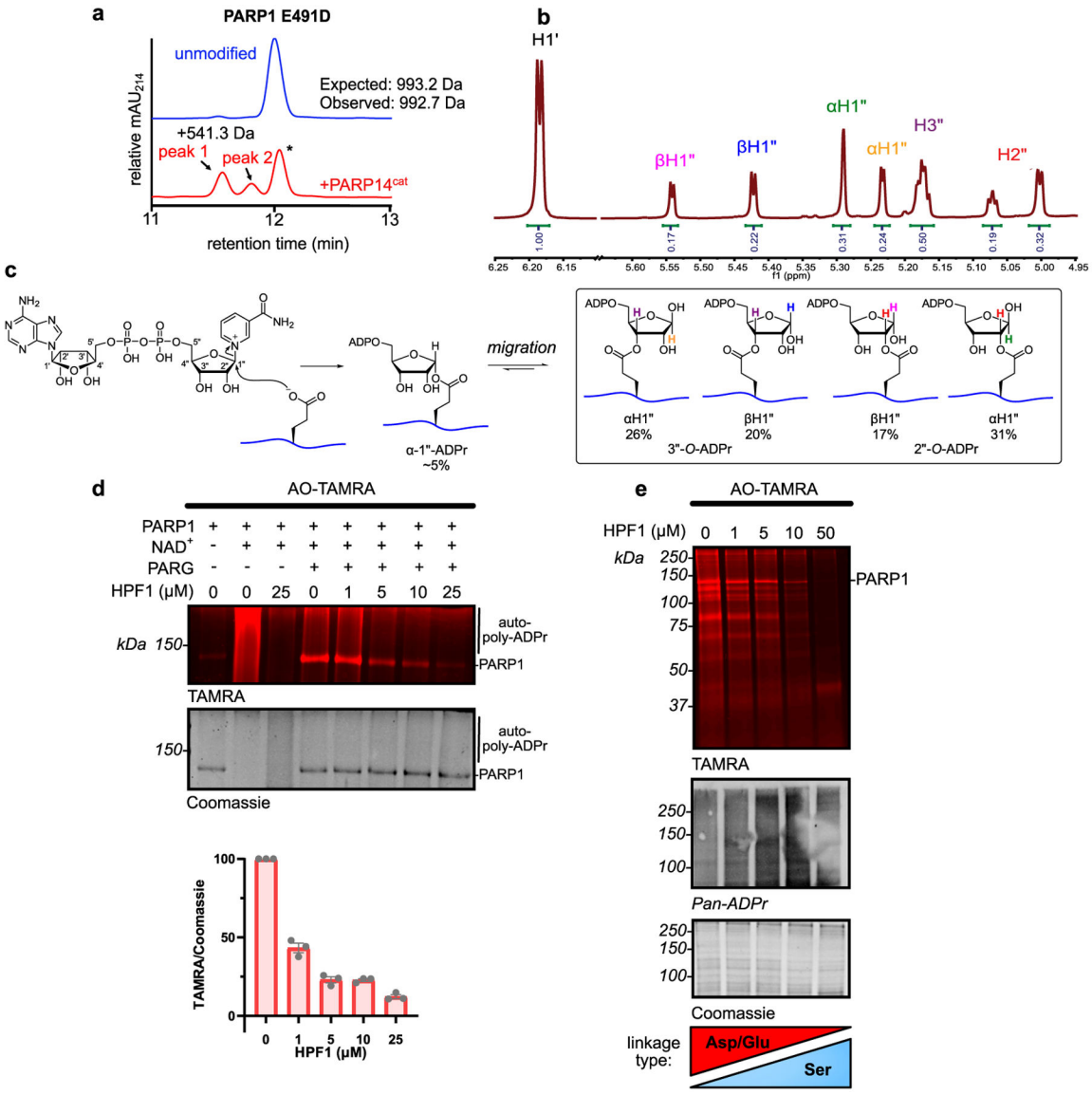

Figure 2.

Structural and biochemical characterization of Asp/Glu-ADPr linkage acyl migration. (a) RP-HPLC/MS analysis of $PARP1_{Frag,\ E491D}$ pre-and postincubation with $PARP14^{cat}$. *Unmodified peptide. (b) ^{1}H-NMR spectrum of $PARP1_{Frag}$ E491ADPr$_1$ peptide. Assigned peaks are labeled with their respective protons. Color corresponds with the different isoforms found in (c). (c) Proposed mechanism for Asp/Glu-ADPr linkage migration and relative isomer abundances derived from integration of the signals as compared to the H-2 signal of the adenosine. (d) Recombinant PARP1 auto-ADPr assays in the presence of increasing HPF1 concentrations. Samples were incubated with AO-TAMRA probe and resolved by SDS-PAGE prior to analysis via in-gel fluorescence imaging or Coomassie staining (top). Poly-ADPr was converted to mono-ADPr via PARG treatment to enable quantification (n = 3, error bars = SD) of AO-TAMRA labeling via densitometry (bottom). (e) ADPr activity in intact nuclei from HEK293T HPF1$^{-/-}$ cells in the presence of increasing concentrations of recombinant HPF1. AO-TAMRA labeling and total ADPr

activity are visualized via in-gel fluorescence and pan-ADPr detection reagent western blot, respectively.

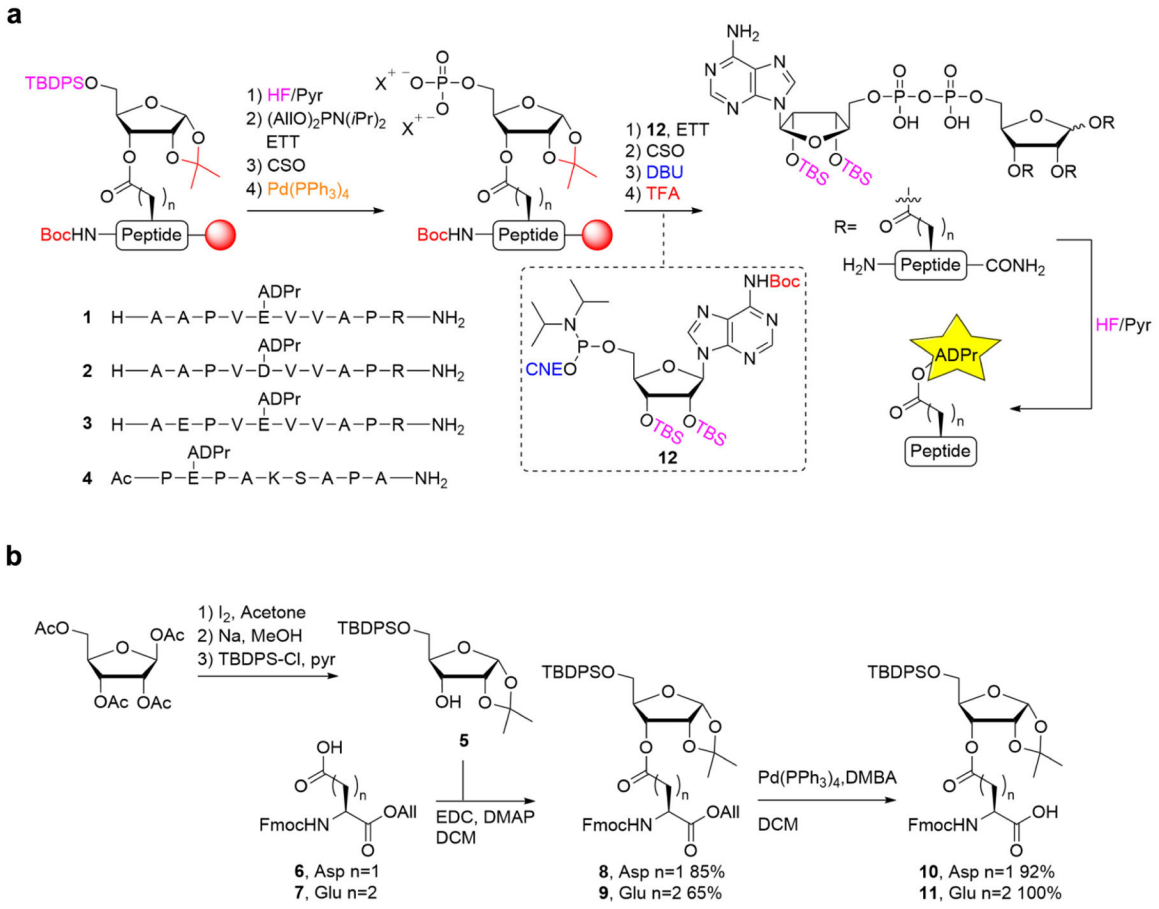

Figure 3.

Total synthesis of Asp/Glu-ADP-ribosylated peptides. (a) Synthetic scheme for on-resin phosphorylation and pyrophosphorylation, resin cleavage, and tandem deprotection to generate various Asp/Glu-ADP-ribosylated peptides (compounds 1–4). Colored protecting groups indicate liability toward the respective deprotection reagent. (b) Synthetic scheme for the protected, ribosylated aspartate (compound 10) and glutamate (compound 11) building blocks that were employed in solid-phase peptide synthesis.

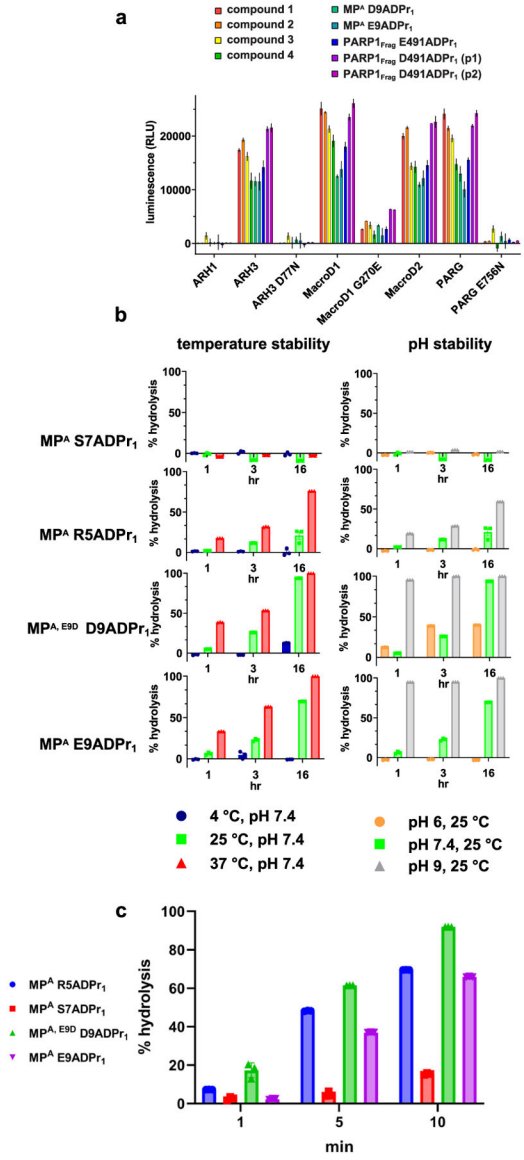

Figure 4.

Enzymatic and nonenzymatic hydrolysis properties of various ADPr linkages. (a) Activity measurements for indicated wild-type and mutant ADP-ribosylhydrolase enzymes with various chemoenzymatically modified and fully synthetic Asp/Glu-ADP-ribosylated substrate peptides. (p1) and (p2) denote peak 1 and peak 2 of Figure 2a, respectively. For all measurements: $n = 3$, error bars = SD. (b) Percent hydrolysis of the indicated ADPr linkage after incubation at various temperatures and pH values as measured by RP-HPLC/MS. For all measurements: $n = 3$, error bars = SD. (c) Percent hydrolysis of the indicated ADPr linkage after incubation in SDS-PAGE sample preparation conditions as measured by RP-HPLC/MS. For all measurements: $n = 3$, error bars = SD.

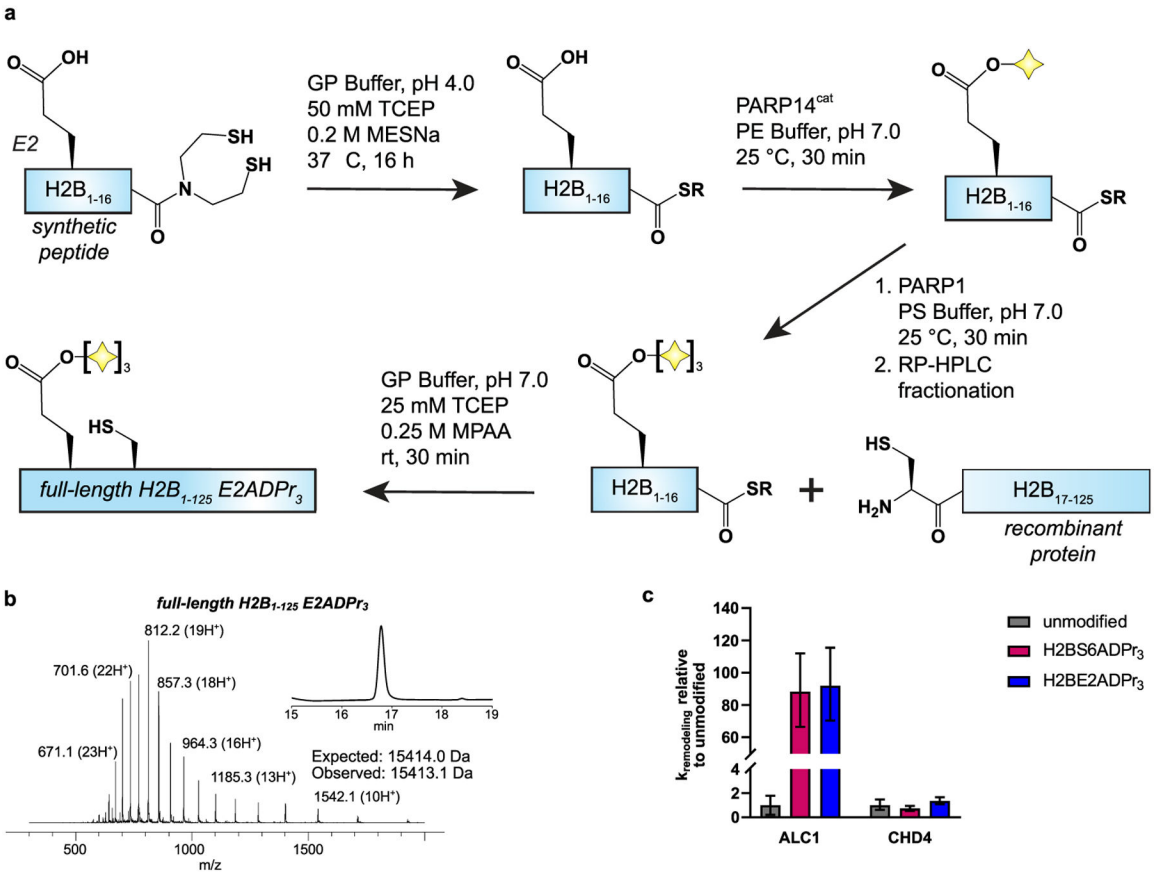

Figure 5.

Semisynthetic nucleosomes bearing histone H2B E2ADPr$_3$ are robust substrates for the chromatin remodeler ALC1. (a) Semisynthetic scheme to prepare full-length H2B E2ADPr$_3$. GP buffer = 6 M guanidine-HCl, 0.1 M sodium phosphate; SR = MES thioester. PE buffer = 50 mM Tris pH 7.0, 20 mM NaCl, 2 mM $MgCl_2$, 10 mM NAD^+. PS buffer = PE buffer supplemented with 10 μM PARP stimulating DNA and 2 mM TCEP. (b) Characterization of the full-length H2B E2ADP3 protein. Raw ESI-MS spectra and RP-HPLC chromatogram are shown. (c) Nucleosome remodeling assay time-course wherein each reaction comprises the indicated remodeler and the indicated nucleosome. "$k_{\text{remodeling}}$ relative to unmodified" is the rate constant of the indicated remodeling reaction relative to that of the unmodified nucleosomes: $n = 3$, error bars = 95% confidence interval.

Table 1.

Af1521 Macrodomain $K_{d,app}$ Values for Arg-, Asp-, Glu-, and Ser-ADP-Ribosylated MPA Peptide Ligands

peptide	$K_{d,app}$ (nM)	SEM (nM)[a]
MP^{A} $R5ADPr_1$	15.6	2.9
$MP^{A\ (R5K,\ E9R)}$ $R9ADPr_1$	28.4	3.4
MP^{A} $S7ADPr_1$	1171.4	691.6
$MP^{A\ (E9D)}$ $D9ADPr_1$	1805.9	435.1
MP^{A} $E9ADPr_1$	732.1	116.0
MP^{A}	n.d.[b]	n.d.
$mp^{A\ (E9D)}$	n.d.	n.d.

[a] Standard error of the mean, $n = 3$.

[b] Binding not detected.